Desalination and Water Treatment
www.deswater.com

doi:10.5004/dwt.2019.24248

160 (2019) 378–387
August

Design and performance measurement of wave-plate mist eliminator with microstructural feature plate surface

Weiwei Ma[a,c], Xiaolin Wu[a,c,*], Zhongli Ji[b,c]

[a]*College of Chemical Engineering, China University of Petroleum, Beijing102249, PR China, email: mavv1989@163.com (W. Ma), wuxl@cup.edu.cn (X. Wu)*
[b]*College of Mechanical and Transportation Engineering, China University of Petroleum, Beijing 102249, PR China, email: jizhongli63@vip.sina.com (Z. Ji)*
[c]*Beijing Key Laboratory of Process Fluid Filtration and Separation, Beijing 102249, PR China*

Received 29 November 2018; Accepted 8 April 2019

ABSTRACT

Wave-plate mist eliminators are widely used to remove airflow droplets in industrial processes. However, with an increase of the gas velocity, a negative impact from re-entrainment becomes obvious and energy consumption from mist eliminator becomes too high. To resolve these problems, a new kind of wave-plate mist eliminator with microstructural features added on the surfaces of wave-plates, is proposed. The effects of microstructural features (triangular, trapezoidal, and square columnar) on mist eliminator drainage performance are experimentally investigated. The separation efficiency and pressure drop of wave-plate mist eliminator are compared and analyzed. The influence of key microstructural dimensional parameters, including microcolumn unit width, circumference center distance spacing, and height, on mist eliminator performance is evaluated. The results indicate that microstructural features significantly increase droplet contact angles on wave-plate surfaces and enhance surface hydrophobicity. The separation efficiency of wave-plate mist eliminator with microstructural features is improved at high gas velocity. The pressure drop of wave-plate mist eliminator with microstructural features is only approximately one-third of pressure drop of a conventional mist eliminator with drainage channels. The three key structural parameters of microcolumn units have a comprehensive effect on mist eliminator performance.

Keywords: Wave-plate mist eliminator; Microstructural feature; Drainage performance; Re-entrainment

1. Introduction

Desalination is widely being adopted as a water treatment process for the generation of fresh water for industrial application. Water droplets should be removed from water vapor generated for controlling salinity levels in the fresh water. Several kinds of mist eliminator have been applied and tested (e.g. filters, cyclones, wire mesh, and wave-plates), of which the choice depends on different operating conditions. Wave-plate mist eliminators are gas-liquid inertial separators with a simple structure, having a lower pressure drop and higher gas throughput compared to other methods that have been widely used in industry [1,2]. The principle of wave-plate mist eliminator is to separate droplets from gas based on differences in inertial forces between the gas and liquid phases. When liquid containing gas stream passes through wave-plate channels, droplets impinge on plate walls to form a liquid film, which then drained by gravity.

An important factor affecting mist eliminator performance is the structural size of the wave-plates. In recent years, many studies have focused on mist eliminator optimization. Monat et al. evaluated the performance of a multi-stage plate with angles of 120° using a laser particle size analyzer [3]. Nakao et al. found that first two stages play a major role in droplet separation, and designed a

*Corresponding author.

simple plate structure with 90° angles [4]. Banitabaei et al. used experimental methods to study wave-plates of simple structures and proposed the best matching relationship between flow path spacing and stage length [5].

However, in practical applications, another more critical factor affecting mist eliminator performance is re-entrainment. Jøsang conducted a theoretical analysis of the mechanism of the re-entrainment [6]. Azzopardi used image grayscale analysis to study horizontal flow wave-plate separators and presented the related the critical Weber number and the re-entrainment critical liquid film thickness [7]. Liquid film thickness on the wave-plate surface is closely related to the occurrence of re-entrainment. Many methods for enhancing wave-plate drainage performance have been proposed to reduce the influence of re-entrainment, with the most common method being the addition of wave-plate drainage channels. James et al. proposed a wave-plate structure with drainage channels and compared it with unaltered structures. The results showed that the addition of drainage channels could significantly decrease the effect of re-entrainment on separation efficiency of mist eliminator [8]. Kavousi and Venkatesan optimized drainage channel size and proposed the best match between drainage channels and runner structures [9,10]. Xu et al. added a thin layer of porous structure on the inner plate wall, which intercepts small droplets and has a stabilizing effect on the liquid film on the wave-plate wall [11].

Most of the earlier researches focused on the drainage channels of wave-plate mist eliminators. In practical industrial applications, the method to add drainage channels on wave-plates can improve the drainage performance of wave-plate mist eliminator and improve separation efficiency. However, the pressure drop of the mist eliminator significantly increases. When there are solid particles in gas steam, mist eliminator often be clogged and fails. To solve this problem, we propose a new method for improving mist eliminator drainage performance by improving wave-plate surface hydrophobicity. There are two main ways to enhance the hydrophobicity of a solid surface, the addition of a low surface energy material as a surface coating and the addition of surface microstructural features. It is difficult to obtain a large-area stable low surface energy film for practical applications. Therefore, a wave-plate mist eliminator with microstructural features which is added to the surfaces of wave-plates has been proposed. In this study, the droplet contact angle and droplet morphology of microstructural wave-plate surfaces were measured, and differences in hydrophobicity among these microstructural surfaces are analysed. Mist eliminator performance with microstructural wave-plates was evaluated and compared with a blank mist eliminator and a mist eliminator containing drainage channel wave-plates. The effects of microstructural critical size parameters on performance were also studied.

2. Experimental details

2.1. Experimental apparatus and procedure

A schematic of the experimental device to test wave-plate mist eliminator performance is shown in Fig. 1. An air-atomizing nozzle, mounted on top of the diffusion chamber, produced a large number of droplets that were initially mixed with air in the diffusion chamber. Some droplets settled in the cavity, while the remaining droplets combined with air entered the horizontal mixing section with the aid of an exhaust fan. The mixing section was 1 m long, which acted to mix the droplets with the air, distributing them more evenly in the airflow and, at the same time, making droplet movement direction and airflow close to horizontal. The mixing section leads to the mist eliminator, whereby the fully mixed liquid-containing gas stream enters the mist eliminator through an inlet with a cross-sectional area of 400 × 120 mm. The mist eliminator is consisted of five wave-plates, forming four horizontal flow channels with spacing of 30 mm. The separated water droplets were collected and weighed. Gas velocity was measured by a Venturi flow meter and controlled at 1.0–10.0 m/s by the

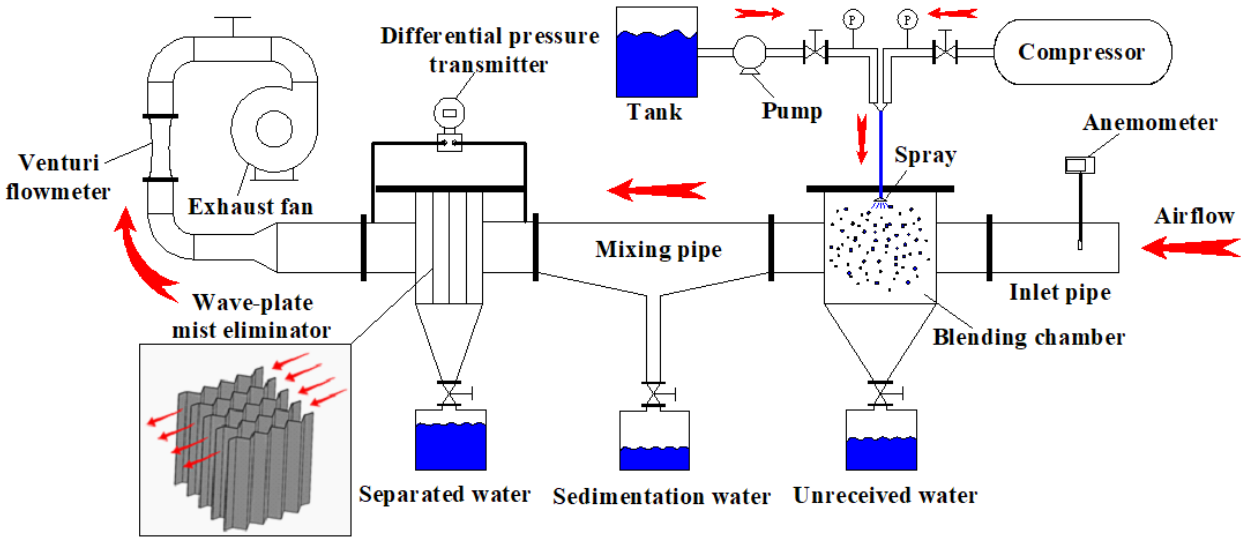

Fig. 1. Schematic diagram of the performance evaluation device for the wave-plate mist eliminator.

fan, fluctuating less than ±0.1 m/s. A hot wire anemometer (0–40 m/s, accuracy class 0.1, Sentry Optronics Co., Ltd, Taiwan, China) was installed at the pipeline inlet, which was verified by comparison with flowmeter results. The airflow Reynolds number was calculated by:

$$Re=\frac{\rho_g u_{g,in} S}{\mu_g} \quad (1)$$

where S is the mist eliminator plate spacing, ρ_g is the air density, $u_{g,in}$ is the velocity, and μ_g is the dynamic viscosity. At atmosphere pressure, ρ_g was 1.226 kg/m^3, and μ_g was 1.79×10^{-5} Pa·s and the range of Re was 2055–18500.

The pressure drop of the mist eliminator was measured using a differential pressure transmitter (accuracy class 0.1, Beckhoff Automation Co., Ltd, Shanghai, China). Pressure points were set at 50 mm from the inlet and outlet sections of the mist eliminator. Due to the large cross-sectional area of the pipeline, the annular pressure acquisition method was adopted to ensure accuracy.

Mist eliminator separation efficiency was measured by the weighing method. The mass of water was weighed by an electronic balance (accuracy class 0.1, Anheng Weighing Apparatus Electronics Co., Ltd, Shenzhen, China), and the value of the separation efficiency η can be calculated by:

$$\eta=\frac{m_4}{m_1-m_2-m_3}\times100\%, \quad (2)$$

where m_1 is the mass of water to the nozzle, m_2 is the mass of unreceived water, m_3 is the mass of sedimentation water, and m_4 is the mass of water separated by wave-plates. To reduce experimental error, the amount of water added in each group of experiments was not less than 5 kg and multiple measurements were averaged. The interior of the experimental device was thoroughly wetted before each experiment to maintain constant humidity.

The droplet size distribution at the nozzle outlet was measured with a Phase Doppler Particle Analyzer (accuracy class 1 grade, Dantec Dynamics A/S, Skovlunde, Denmark), according to the light scattering effects of moving particles as shown in Fig. 2.

As the droplet distribution at the nozzle outlet is conical, 120 measurement points were evenly arranged on three parallel sections for accurate measurement as shown in Fig. 3. Fig. 4 illustrates the droplet size distribution at the nozzle outlet was 15–210 μm at 0.3 MPa water pressure and 0.3 MPa air pressure. The mass distribution of each particle size was relatively uniform, which is consistent with the wide droplet size distribution, high concentration of the gas stream, and large droplets in the gas stream.

The contact angle of the droplets on the surface of the microstructure and the shape of the droplets were measured using the Theta Lite TL100 contact angle meter (Biolin Scientific Co., Ltd. Swedish).

2.2. Design of the wave-plate mist eliminator

In practical industrial applications, re-entrainment is the key factor affecting the performance of wave-plate mist eliminator, especially at high gas velocity. There are four known mechanisms with which new droplets are generated. The mechanisms can be classified into the following groups, representing the origin of the new droplets: (a) Droplet-droplet interaction, (b) droplet breakup, (c) splashing of the impinging droplet, and (d) re-entrainment from the liquid film. The breakup of droplets by impingement on liquid film and re-entrainment from liquid film are the most important mechanism for the generation of the secondary

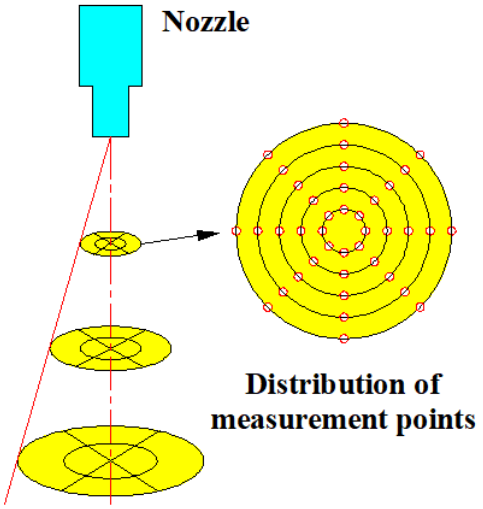

Fig. 3. Schematic diagram of the distribution of measurement points.

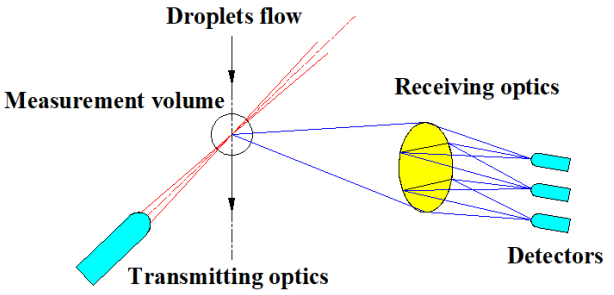

Fig. 2. Schematic diagram of the phase doppler particle analyzer optical path.

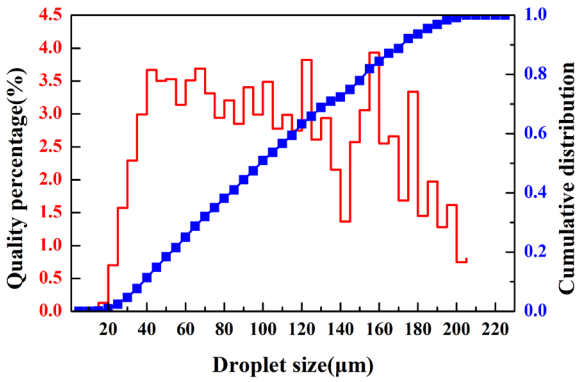

Fig. 4. Droplet particle size distribution at the nozzle outlet.

droplets. Re-entrainment from liquid film can be estimated using the Weber number:

$$We=\frac{\rho_g\left(u_{g,in}-u_f\right)^2 h_{lf}}{\sigma} \tag{3}$$

where ρ_g is the gas density, u_f is the velocity of liquid film, h_{lf} is the characteristic thickness of the liquid film, and σ is the surface tension coefficient. A larger Weber number indicates that the inertial force is more effective than the surface tension, and therefore more likely to cause re-entrainment. It can also be seen from the above formula that the Weber number is mainly affected by two factors: the gas-liquid phase velocity difference and liquid film characteristic thickness. Therefore, when the gas-liquid phase velocity difference is constant, reducing the liquid film thickness is an effective method for suppressing re-entrainment.

The most common method to reduce the thickness of liquid film is increasing the surface hydrophobicity. At present, the droplet contact surface angle of a surface material with the lowest surface energy is only 120° [12]. In order to obtain a larger liquid contact angle at surface, it is necessary to add microstructural features to the surface. Many researches have examined the hydrophobic mechanism and acquisition methods of microstructural surfaces [13–17].

In this research, three of the most common microstructural features (triangular, trapezoidal, and square columnar) were added to the surface of wave-plates as depicted in Fig. 5. According to the Wenzel model, microstructural surface roughness has an important influence on its hydrophobic properties. The calculation formula was

$$r=4\varphi\frac{h}{a}+1 \tag{4}$$

$$\varphi=\left(\frac{a}{l}\right)^2 \tag{5}$$

where r is the microstructure surface roughness, and ϕ is the microstructure area fraction. The variables a, l, and h are the width, center distance, and height of the microcolumn unit, respectively. Therefore, a, l, and h are considered to be the main geometric parameters of microstructural design. The height and width of microcolumn elements are equal to 0.5 mm for all three microstructural features.

Wave-plate mist eliminators are typically constructed from a series of L-shaped or zigzag wave-plates. In this study, a wave-plate with 90° angle and 60 mm in length was selected as the substrate. Hydrophobic microstructural features were added to the inner surfaces of flow channel. A wave-plate with the same structural parameters and additional drainage channels was selected for comparison as is indicated in Fig. 6.

3. Results and discussion

3.1. Contact angle

Wave-plate surfaces were hydrophobically modified using the above-mentioned three types of microstructural feature (triangular, trapezoidal, square cylindrical). Surface droplet contact angles and droplet states are two important criteria for measuring hydrophobicity. On blank wave-plate surfaces, the initial droplet contact angle is about 93.37°, showing very weak hydrophobicity as depicted in Fig. 7. After hydrophobic modification, the droplet contact angles on the triangular, trapezoidal, and square cylindrical microstructural surfaces are 118.03°, 109.13°and 123.50°, respectively. Compared to the blank surface, the droplet contact angle of all three microstructural surfaces significantly

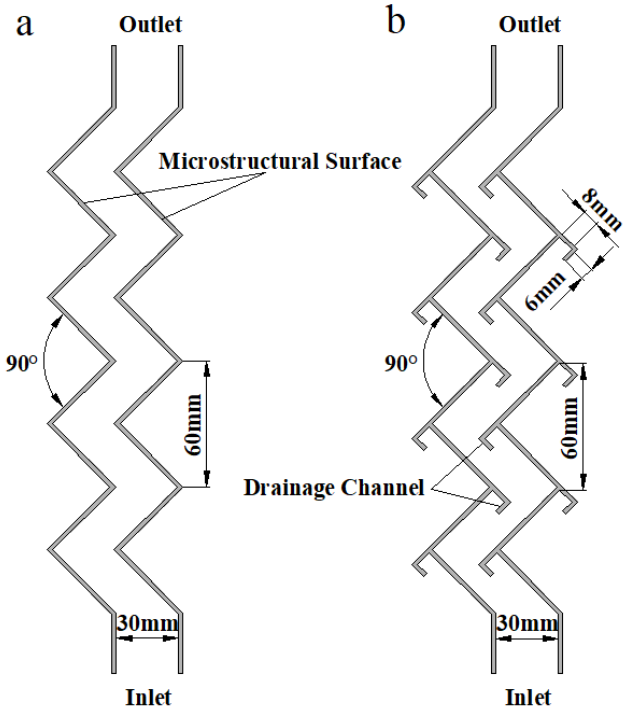

Fig. 6. Structural parameters of mist eliminator flow path: (a) microstructural surface wave-plates and (b) wave plates with drainage channels.

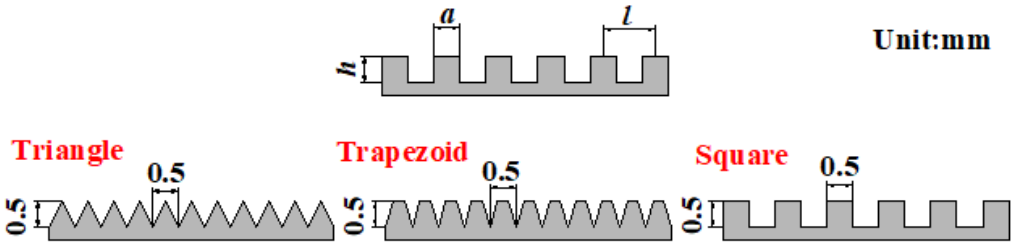

Fig. 5. Schematic diagram of microcolumn structure.

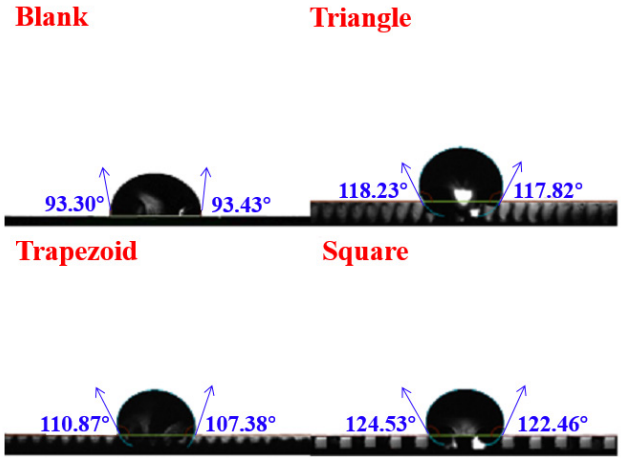

Fig. 7. Effects of different microcolumn units on surface droplet contact angle.

increase, and the hydrophobicity of wave-plate surface is enhanced.

The droplets on the triangular and trapezoidal microcolumn units are in the Wenzel state, while droplet on the square cylindrical microcolumn unit is close to the Cassie state. The Wenzel state and Cassie state are two different morphology of droplet on microstructural surface, and the theoretical models of them are shown in Fig. 8. In the Cassie state, the droplet is located on top of the microstructural surface with trapped air underneath. In the Wenzel state, the air pockets are no longer thermodynamically stable and liquid begins to nucleate from the middle of the droplet, creating a "mushroom state". Commonly, in order to obtain the best hydrophobic performance, the droplet on microstructure surface can be controlled to keep in the Cassie state. The state of droplet on microstructural surface can be judged by the following two critical parameters: the critical contact angle of droplet (θ_{cr}) and the minimum height of microcolumn unit (H_{min}). If the contact angle of droplet is larger than the critical angle, the droplet exhibits the Cassie state. If the height of the microcolumn unit is larger than the minimum height, it is can be ensured that the liquid bending surface at the bottom of droplet does not contact with the bottom of the microstructure. The condition is given by:

$$\cos\theta_{cr} = \frac{1-\varphi}{\varphi - r} \tag{6}$$

$$H_{min} = \sqrt{2}(l-a)\frac{\sin\theta - 1}{2\cos\theta} \tag{7}$$

where θ is the droplet contact angle, θ_{cr} is the critical contact angle of droplet, and H_{min} is the minimum height of microcolumn unit. By putting the Eqs. (4), (5) into the Eqs. (6), (7), the critical contact angle of droplet and the minimum height of microcolumn unit can be calculated. As a is 0.5 mm, l is 1.0 mm, and h is 0.5 mm, θ_{cr} is about 115°, and H_{min} is about 0.1 mm.

In conclusion, the droplet contact angle on the square cylindrical microcolumn unit is 123.50° > 115°and the droplet contact angle on the trapezoidal microcolumns unit is 109.13° < 115°. It is shown that the droplet on the square cylindrical microcolumn unit is in the Cassie state and the droplet on the trapezoidal microcolumn unit is in the Wenzel state. On the other hand, compared with the vertical wall structure, triangular unit with inclined walls shows poor surface droplet stability and droplet is more likely to flow into the gap and turns into the Wenzel state, which resulted in the droplet contact angle on the triangular microcolumn unit is smaller than that on the square cylindrical microcolumn unit. Therefore, the square cylindrical microcolumn unit has the most obvious effect by comparing the droplet contact angle.

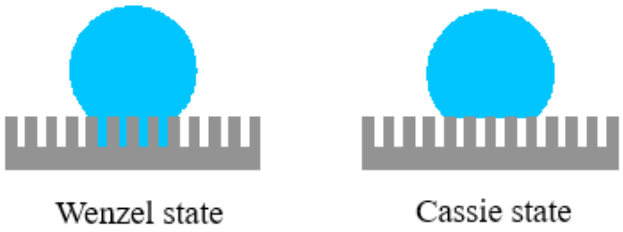

Fig. 8. Theoretical models of Wenzel state and Cassis state.

3.2. Overall separation efficiency

The gas-liquid separation efficiency of the mist eliminator is an important criterion for evaluating its performance. The efficiency of the wave-plate mist eliminator with different microstructural features were compared with the blank mist eliminator and the mist eliminator with drainage channels, and the result is indicated in Fig. 9. As it can be observed, the separation efficiency increases with increasing gas velocity in range 1.0–4.0 m/s due to the increased the inertia force exerted on the droplet. Adding microstructural features on the wave-plate surface increases the separation efficiency of mist eliminator at 5–10%, and the effect of three kinds of microstructural feature are almost the same. However, improvement of the separation efficiency of mist eliminator by the drainage channels is slightly higher than that of microstructural surfaces. The reason is that, at low gas velocities, droplet inertia in the gas stream is small, but setting the drainage channels reduces the spacing of the mist eliminator flow path, which causes the increase of droplet inertial force and makes it more facile for droplets to hit the wall. At the same time, drainage channels also have interception effect on nearby droplets. The above two factors improve the overall performance of the mist eliminator. On the other hand, the main effect of microstructural surface is to enhance the drainage performance of the mist eliminator, but it has no direct enhancement effect on droplet interception. When the gas velocity is low, re-entrainment does not occur, and the drainage performance of the wave-plate mist eliminator has little influence on its overall performance.

With continued increase in the velocity above 5 m/s, re-entrainment begins to occur, resulting in a decrease of the separation efficiency for all three mist eliminators. As depicted in Fig. 10, large droplet splashes downstream of the mist eliminator are clearly observed, and the influence of drainage performance of the mist eliminator becomes significant in this condition. This indicates that the separation efficiency of the mist eliminator with square cylindrical microstructural feature is substantially the same as the mist

eliminator with drainage channels at high gas velocity. The separation efficiency of the mist eliminator with the other two microstructural features are slightly lower. Compared to the mist eliminator with enhanced drainage structures, the separation efficiency of the blank mist eliminator decreases more significantly at high gas velocity. When the mist eliminator drainage performance is enhanced, the liquid film on flow channel inner wall becomes thinner, which reduces the influence of re-entrainment on separation efficiency of mist eliminator, consistent with the results of Azzopardi et al. [7].

3.3. Pressure drop

Pressure drop in the mist eliminator is largely related to the energy consumption of the entire system. During the separation process, airflow flows through the downstream portion of the corner of the mist eliminator flow channel, and creates several reflux zones [18]. As these reflux zones reduce the width of the local flow channel and increases droplet inertial forces, the separation efficiency and pressure drop of wave-plate mist eliminator are affected.

The Euler number is usually used as a dimensionless number to describe pressure drop of the mist eliminator, which is calculated as

$$Eu = \frac{\Delta p}{\rho_g u_{g,in}^2} \tag{8}$$

where Δp is the pressure difference between the mist eliminator inlet and outlet. The Euler number Eu reflects the relationship between the liquid phase pressure and inertial force.

The functional relationship between the internal Reynolds number and Euler number of the mist eliminator with microstructural wave-plates was obtained and compared to mist eliminators with blank wave-plates or with drainage channel wave-plates. The Euler number of the blank mist eliminator is the smallest when the conditions are held constant as is shown in Fig. 11. In contrast, the mist eliminator with the drainage channels has the highest Euler number. When drainage channels are used for enhancing drainage performance, the width of the flow channel nearby the drainage channels are decreased

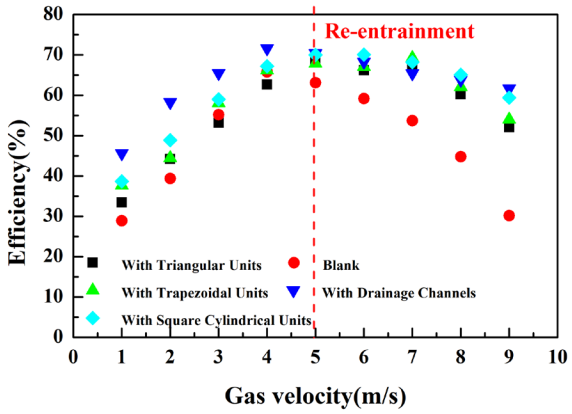

Fig. 9. Effects of microstructural features and drainage channels on the separation efficiency of mist eliminator at different gas velocities.

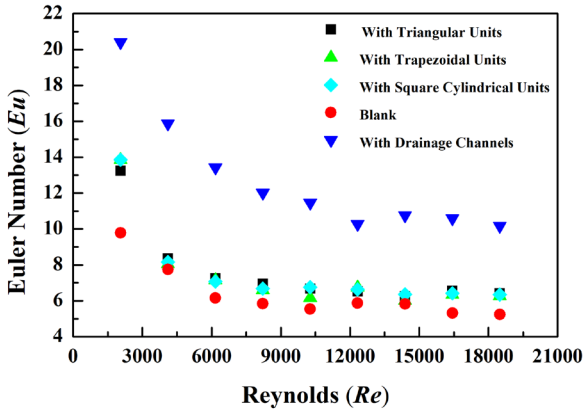

Fig. 11. Effects of microstructural features and drainage channelson mist eliminator pressure drop at different Reynolds number.

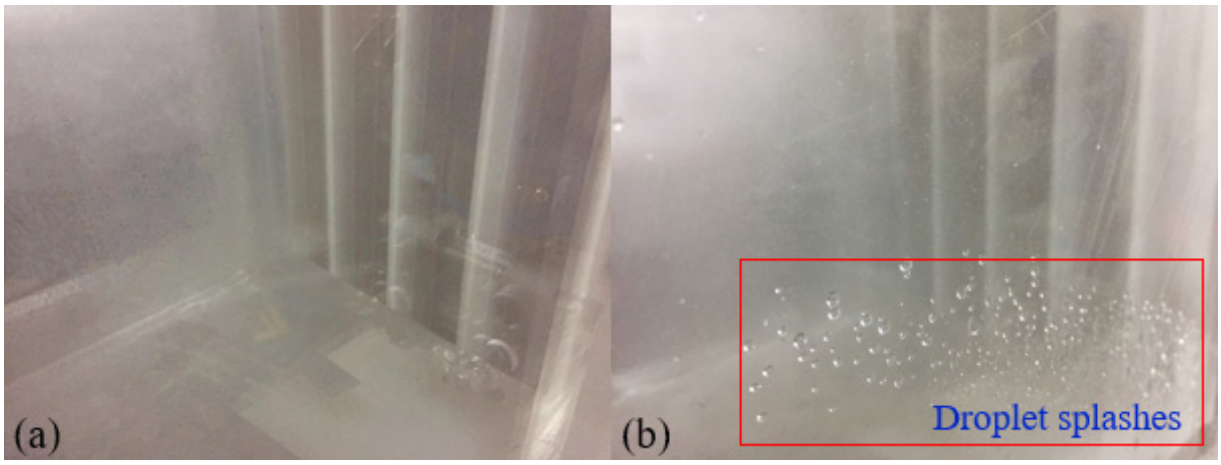

Fig. 10. Pictures of droplet splashes: (a) re-entrainment does not occur at low gas velocity; (b) re-entrainment occurs at high gas velocity.

sharply which leads to separation of airflow boundary layer. Moreover, vortexes at the inlet and inside the drainage channels increase the local resistance of airflow. The Euler number of the mist eliminator for all three microstructural features are nearly the same. They are higher than the Euler number of blank mist eliminator, and are much smaller than the Euler number of the mist eliminator with drainage channels. Due to the small size of the microstructural features, their influence on the airflow boundary layer inside the flow channel is limited, and the energy loss from them is low. Combined with the results discussed in section 3.2, it is shown that the separation efficiency of the mist eliminator with microstructural features is similar to the separation efficiency of traditional mist eliminator with drainage channels. However, the effects of the two drainage enhanced structures on pressure drop of the mist eliminator are quite different.

3.4. Parameters of microstructure

Mist eliminator drainage performance is affected by the hydrophobicity of internal wave-plate surfaces. Surface roughness is the most important factor determining the hydrophobicity of these surfaces. The dimensional change of the microcolumn unit structure directly changes wave-plate surface roughness, thereby affecting the overall mist eliminator performance. Considering comprehensively the effects of the three kinds of microstructural features, the square cylindrical microstructural feature most clearly improves the hydrophobicity of the wave-plate surface. Thus, taking the square cylindrical microstructural feature as example, the microcolumn unit width a, centre distance l, and height h of a series of samples were measured as is shown in Table 1.

As depicted in Fig. 12, the efficiency and pressure drop of samples (#1, #2, and #7) with the three microcolumn units with center distances and heights of 1.0 mm are compared. When the gas velocity is less than 5 m/s, the efficiency of the three samples are almost the same. When the gas velocity is further increased, re-entrainment begins to occur, and the mist eliminator with the smallest a of the microcolumn unit has the higher separation efficiency. Under the same conditions, the contact angle of the droplets on the surface of the wave-plate increases and the hydrophobicity increases, as a becomes smaller. This is consistent with the results of Song et al. [19]. Comparing surfaces of wave-plates of the same size, the smaller the a of the microcolumn, the larger the number of grooves between the microcolumn units within the unit width, and the greater the influence on airflow at the boundary layer. Therefore, pressure drop of the mist eliminator is higher.

The effects of microcolumn unit center distance are evaluated by comparing samples #3, #4, and #5 as shown in Fig. 13. When the height of the microcolumn unit is constant, the droplet contact angle increases with the increase of the center distance of the microcolumn unit [19], and the efficiency

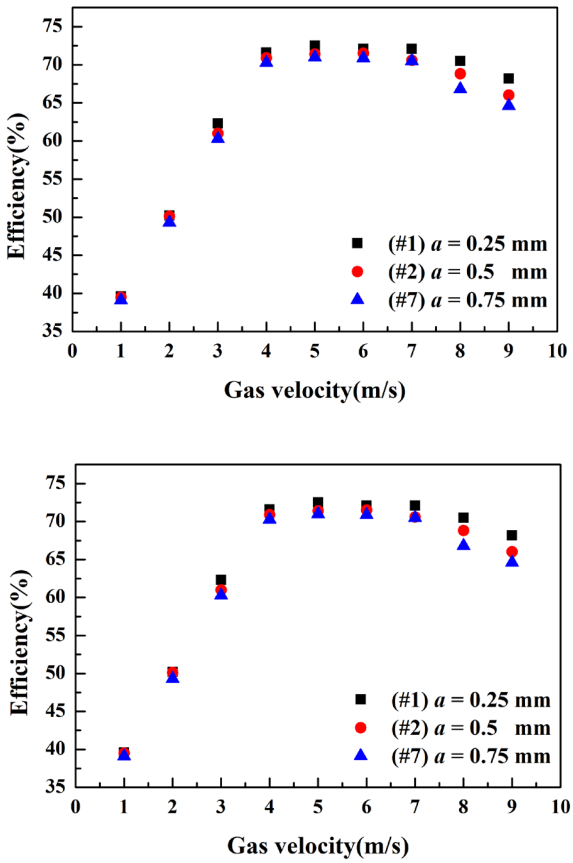

Fig. 12. Effects of microcolumn unit width on mist eliminator performance.

Table 1
Wave-plate microstructure unit size parameters

Sample No.	Unit width a (mm)	Unit spacing l (mm)	Unit height h (mm)	Area fraction ϕ (%)	Roughness r
#1	0.25	1.0	1.0	0.06	2.0
#2	0.5	1.0	1.0	0.25	3.0
#3	0.5	1.0	0.5	0.25	2.0
#4	0.5	1.25	0.5	0.16	1.6
#5	0.5	1.5	0.5	0.11	1.4
#6	0.5	1.0	0.25	0.25	1.5
#7	0.75	1.0	1.0	0.56	4.0

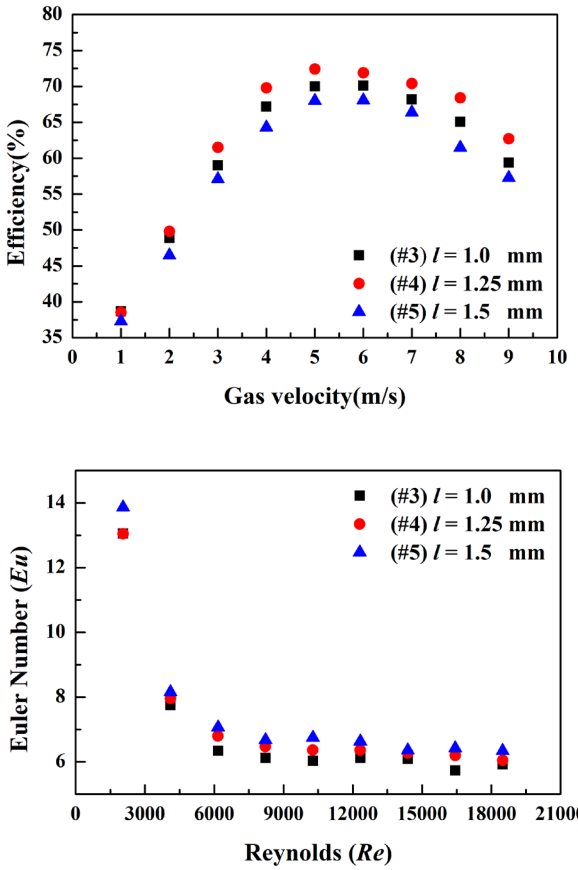

Fig. 13. Effects of microcolumn units center distance on mist eliminator performance.

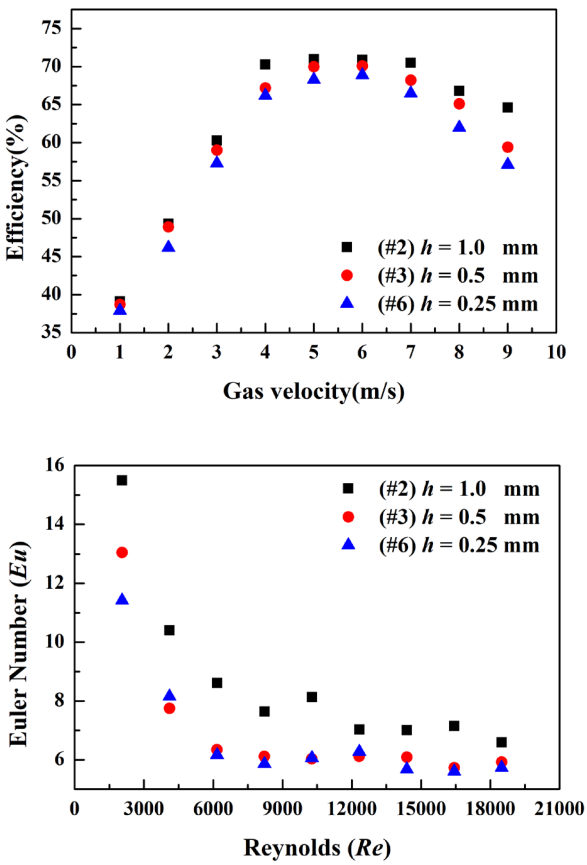

Fig. 14. Effects of microcolumn unit height on mist eliminator performance.

of #4 is higher than that of #3 at the same gas velocity. However, the efficiency of sample #5 is lowest with a larger center distance. When the spacing of microcolumn cells is too large, the sinking distance of the droplets on the surface in the height direction is larger than the microcolumn height. The droplets contact the bottom surface of the microstructures, and the Cassie state of droplets are destroyed which leads to a decrease in hydrophobicity of microstructural surface. Pressure drop of the three samples are similar and the center distance of the microcolumn has little effect on pressure drop of the mist eliminator.

Fig. 14 illustrates the effect of the microcolumn units on the performance of wave-plate mist eliminator for sample #2, #3, and #6. The higher the height of the microcolumn unit, the more hydrophobic, and the mist eliminator has better drainage performance, especially at high gas velocity. However, an increase in the microcolumn unit height significantly increases pressure drop of the mist eliminator.

3.5. Correlation of the experimental data

In former discussion, the wave-plate microstructure unit width (a), center distance (l), and height (h) and gas velocity (v) influence to the separation efficiency and the pressure drop of wave-plate mist eliminator is investigated. Empirical correlations stated below can be obtained by fitting experimental data using least square method:

$$\eta = 40.045 \times a^{0.006} l^{0.019} h^{0.059} v^{0.315} \quad (9)$$

$$\Delta p = 16.119 \times a^{-0.139} l^{-0.064} h^{0.246} v^{1.639} \quad (10)$$

Fig. 15 shows the comparison between measured and calculated values for separation efficiency and pressure drop, respectively. The correlation relation of them can be used to evaluate the separation efficiency and the pressure drop with an accuracy about ±5%.

4. Conclusions

A new kind of wave-plate mist eliminator with microstructural features added on the surface of wave-plates was designed and fabricated. The droplet contact angle and droplet state of wave-plate surfaces with microstructural features were measured. The effects of microstructural features on mist eliminator drainage performance and overall mist eliminator performance were compared and analysed. The influence of the key dimension parameters of the microstructure on mist eliminator performance was measured. The following conclusions are obtained:

The addition of microstructural features on wave-plate surfaces can effectively increase the contact angle of surface droplets, thereby enhancing hydrophobicity of the wave-plate surface. The droplet contact angle of

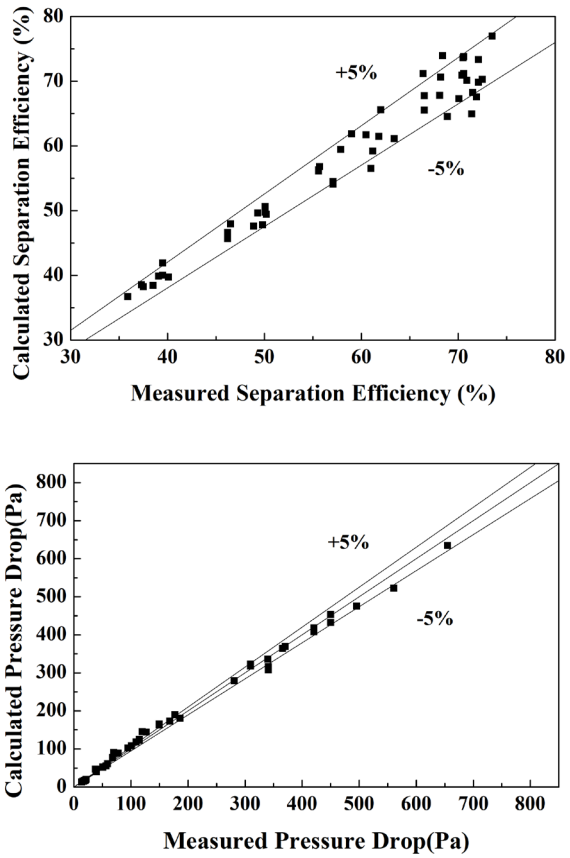

Fig. 15. Comparison between measured and calculated values for separation efficiency and pressure drop.

the square cylindrical microcolumn unit surface is larger than that of the triangular and trapezoidal microcolumn unit surfaces. Droplets on the triangular and the trapezoidal microcolumn units exhibit the Wenzel state, while droplet on the square cylindrical microcolumn unit is close to the Cassie state. The square cylindrical microcolumn is more effective than the triangular and trapezoidal microcolumns.

Adding the microstructural features, the drainage performance of wave-plate mist eliminator is improved, and the adverse effects caused by re-entrainment at high gas velocity is suppressed. In terms of improving the separation efficiency of the mist eliminator, the effect is similar to the conventional method of adding drainage channels. However, the pressure drop of microstructural features is far lower than that of the drainage channels. As a result, this new kind of wave-plate mist eliminator is more economical than conventional ones.

The three key structural parameters of the microcolumn units have a comprehensive effect on mist eliminator performance, a and h are particularly influential. The mist eliminator separation efficiency increases as a and h decrease. As the spacing of the microcolumn increases, the separation efficiency initially increases, then it decreases. Pressure drop of the mist eliminator decreases as a increases, and increases as l and h increase. Two empirical correlations with accuracy of ±5% were obtained by fitting the experimental data, which can be used for predicting separation efficiency and pressure drop of the wave-plate mist eliminator for our selected microstructureal features and experiment conditions.

Acknowledgments

The authors acknowledge the financial support of National Natural Science Foundation of China (No.51474229).

Symbols

r — Microstructure surface roughness (dimensionless)
ϕ — Microstructure area fraction (dimensionless)
a — Microcolumn unit width (mm)
l — Microcolumn unit center distance (mm)
h — Microcolumn unit height (mm)
Re — Reynolds number (dimensionless)
ρ_g — Air density (kg/m^3)
$u_{g,in}$ — Air velocity (m/s)
μ_g — Air dynamic viscosity (Pa·s)
S — Mist eliminator plate spacing (mm)
m_1 — Nozzle water quality (kg)
m_2 — Unreceived water quality (kg)
m_3 — Sedimentation water quality (kg)
m_4 — Mass of water separated by the wave-plate (kg)
We — Weber number (dimensionless)
u_f — Velocity of liquid film (m/s)
h_{lf} — Characteristic thickness of the liquid film (mm)
σ — Surface tension coefficient (dimensionless)
Eu — Euler number (dimensionless)
θ — Droplet contact angle (°)
θ_{cr} — Critical contact angle of droplet (°)
H_{min} — Minimum height of microcolumn unit (mm)
η — Separation efficiency of wave-plate mist eliminator (%)
Δp — Pressure difference between the mist eliminator inlet and outlet (Pa)

References

[1] J. Li, S.Y. Huang, X.M. Wang, J.J. Kuang, Experimental research of cold state operation of corrugated-plate separator, J. Huazhong Univ. Sci. Technol. Nat. Sci. Ed., 36(1) (2008) 112–114.
[2] P.L. Xia, J. Yang, Performance analysis and research progress of wave-plate mist eliminator, Process. Equip. Piping, 50(6) (2013) 33–36.
[3] J.P. Monat, K.J. McNulty, I.S. Michelson, Accurate evaluation of chevron mist eliminators, Chem. Eng. Prog., 82(12) (1986) 32–39.
[4] T. Nakao, M. Nagase, G. Aoyama, M. Murase, Development of simplified wave-type vane in BWR steam dryer and assessment of vane droplet removal characteristics, J. Nucl. Sci. Technol., 36(5) (1999) 424–432.
[5] S.A. Banitabaei, H. Rahimzadeh, R. Rafee, Determination of minimum pressure drop at different plate spacings and air velocity in a wave-plate mist eliminator, Asia-Pac. J. Chem. Eng., 7(4) (2012) 590–597.
[6] A.I. Jøsang, Numerical and experimental studies of droplet-airflow, Ph.D. Thesis, Faculty of Engineering Science and Technology, Norwegian University of Science and Technology, 2002.

[7] B.J. Azzopardi, K.S. Sanaullah, Re-entrainment in wave-plate mist eliminators, Chem. Eng. Sci., 57(17) (2002) 3557–3563.
[8] P.W. James, Y. Wang, B.J. Azzopardi, J.P. Hughes, The role of drainage channels in the performance of wave-plate mist eliminators, Chem. Eng. Res. Des., 81(6) (2003) 639–648.
[9] F. Kavousi, Y. Behjat, S. Shahhosseini, Optimal design of drainage channel geometry parameters in vane mist eliminator liquid–gas separators, Chem. Eng. Res. Des., 91(7) (2013) 1212–1222.
[10] G. Venkatesan, N. Kulasekharan, S. Iniyan, Design and selection of curved vane mist eliminators using Taguchi based CFD analysis, Desalination, 354 (2014) 39–52.
[11] Y.C. Xu, Z.M. Yang, J.S. Zhang, Study on performance of wave-plate mist eliminator with porous foam layer as enhanced structure. Part II: Experiments, Chem. Eng. Sci., 171 (2017) 662–671.
[12] T. Nishino, M. Meguro, K. Nakamae, M. Matsushita, The lowest surface free energy based on – CF3 alignment, Langmuir, 15(13) (1999) 4321–4323.
[13] M.F. Zhu, W.W. Zuo, H. Yu, W. Yang, Y.M. Chen, Superhydrophobic surface directly created by electrospinning based on hydrophilic material, J. Mater. Sci., 41(12) (2006) 3793–3797.
[14] L.L. Cao, H.H. Hu, D. Gao, Design and fabrication of micro-textures for inducing a superhydrophobic behavior on hydrophilic materials, Langmuir, 23(8) (2007) 4310–4314.
[15] J.L. Liu, X.Q. Feng, G.F. Wang, S.W. Yu, Mechanisms of super hydrophobicity on hydrophilic substrates, J. Physics: Condensed Matter, 19(35) (2007) 356002.
[16] Z. Guo, W. Liu, Biomimic from the super hydrophobic plant leaves in nature: Binary structure and unitary structure, Plant Sci., 172(6) (2007) 1103–1112.
[17] R. Blossey, Self-cleaning surfaces—virtual realities, Nat. Mater., 2(5) (2003) 301.
[18] C.C.J. Verlaan, Performance of novel mist eliminators, Ph.D. Thesis, aan de Technische Universiteit Delft, 1991.
[19] H. Song, Z.Q. Liu, X.Y. Shi, Y.K. Cai, Model of contact angle of hydrophobic surface based on minimum Gibbs free energy, J. Shandong Univ.: Eng. Sci., 45(2) (2015) 56–61.